

Conditional Eulerian and Lagrangian velocity increment statistics of fully developed turbulent flow

Holger Homann^{1,2}, Daniel Schulz¹, and Rainer Grauer^{11, a)}

¹ *Theoretische Physik I, Ruhr-Universität, 44780 Bochum, Germany*

² *Université de Nice-Sophia Antipolis, CNRS, Observatoire de la Côte d'Azur, Laboratoire Cassiopée, Bd. de l'Observatoire, 06300 Nice, France*

(Dated: 28 October 2018)

Conditional statistics of homogeneous isotropic turbulent flow is investigated by means of high-Reynolds number direct numerical simulations performed with 2048³ collocation points. Eulerian as well as Lagrangian velocity increment statistics under several conditions are analyzed and compared. In agreement with experimental data longitudinal probability density functions $P(\delta_l^{\parallel} u | \epsilon_l)$ conditioned on a scale-averaged energy dissipation rate are close to Gaussian distributions over all scales within the inertial range of scales. Also transverse increments conditioned on either the dissipation rate or the square of the vorticity have quasi-Gaussian probability distribution functions (PDFs). Concerning Lagrangian statistics we found that conditioning on a trajectory averaged energy-dissipation rate ϵ_τ significantly reduces the scale dependence of the increment PDFs $P(\delta_\tau u_i | \epsilon_\tau)$. By means of dimensional arguments we propose a novel condition for Lagrangian increments which is shown to reduce even more the flatness of the corresponding PDFs and thus intermittency in the inertial range of scales. The conditioned Lagrangian PDF corresponding to the smallest increment considered is reasonably well described by the K41-prediction of the PDF of acceleration. Conditioned structure functions show approximately K41-scaling with a larger scaling range than the unconditioned ones.

Keywords: Homogeneous isotropic turbulence, conditional statistics, intermittency

I. INTRODUCTION

The problem of anomalous scaling can be seen as one of the great unsolved problems in turbulence research. The scaling laws of velocity structure functions $S_p(l) = \langle (\delta_l u)^p \rangle \sim l^{\zeta_p}$ within the inertial range of scales of fully developed turbulence has inspired a lot of publications over the last decades^{1,2}. The velocity increment under consideration is usually either the longitudinal $\delta_l^{\parallel} u = (\mathbf{u}(\mathbf{x} + \mathbf{l}) - \mathbf{u}(\mathbf{x})) \cdot \hat{\mathbf{l}}$ or the transverse one $\delta_l^{\perp} u = |(\mathbf{u}(\mathbf{x} + \mathbf{l}) - \mathbf{u}(\mathbf{x})) \times \hat{\mathbf{l}}|$. Both are so called Eulerian increments because the velocity differences are taken over spatial separations at a the same instant of time. Kolmogorov's K41-theory³ implies a linear scaling law $\zeta_p = p/3$ not distinguishing between the two different types of increments mentioned before. However, direct numerical simulations (DNS) and experiments show a deviation of the form¹

$$\zeta_p = p/3 - \mu_p, \quad (1)$$

with a positive μ_p . The question whether longitudinal and transverse statistics possesses two different sets of scaling exponents ζ_p^{\parallel} , ζ_p^{\perp} respectively, is still under discussion. Experimental observations^{4,5} as well as DNS⁶ found slightly smaller scaling exponents for the high-order transverse than for the longitudinal structure functions. It is not yet clear whether these findings are finite-Reynolds number and/or anisotropy effects. In the case

of election-MHD turbulence⁷ the differences between longitudinal and transverse scaling exponents were found to decrease with Reynolds-number. One has also to be very careful in the determination of these scaling exponents⁸ as longitudinal and transverse structure functions possess differing scaling ranges.

Guided by Kolmogorov's refined self similarity hypothesis⁹ (RSH)

$$\delta_l^{\parallel} u = \beta_1 (\epsilon_l l)^{\frac{1}{3}} \quad (2)$$

which states a relation between the local energy dissipation rate

$$\epsilon(\mathbf{x}) = \nu \sum_{i,j} [\partial_j u_i(\mathbf{x}) + \partial_i u_j(\mathbf{x})]^2 \quad (3)$$

averaged over a scale l

$$\epsilon_l = \frac{1}{l} \int_0^l \epsilon(\mathbf{x} + s \hat{\mathbf{l}}) ds \quad (4)$$

(l indicating the same line appearing in $\delta_l^{\parallel} u$ and $\delta_l^{\perp} u$) and the velocity fluctuation $\delta_l^{\parallel} u$ over that scale Gagne et Ac.¹⁰ experimentally measured conditional velocity increment statistics. They found the probability density functions (PDFs) $P(\delta_l^{\parallel} u | \epsilon_l)$ to be nearly Gaussian from the dissipation- up to the integral-scale which implies a linear scaling law with $\mu_p = 0$ in (1). It is believed that anomalous scaling ($\mu_p \neq 0$) in turbulent flows has its origin in small-scale intermittency of the local energy dissipation rate. This point of view is supported by this result, namely that the statistics of increments become

^{a)} Electronic mail: holger@tp1.rub.de

Gaussian once they are conditioned on a scale-averaged energy dissipation rate.

Recently, new experimental techniques have provoked a renewed interest in Lagrangian statistics^{11–13}. Here, velocity increments are taken along trajectories of fluid elements (tracers). Lagrangian velocity increments are defined by

$$\begin{aligned} \delta_\tau v_i &= v_i(\tau) - v_i(0) \\ &= u_i(\mathbf{X}(\mathbf{x}_o, \tau), \tau) - u_i(\mathbf{X}(\mathbf{x}_o, 0), 0), \end{aligned} \quad (5)$$

where $\mathbf{X}(\mathbf{x}_o, \tau)$ denotes the trajectory of a tracer which started at the position \mathbf{x}_o at time $t = 0$. Although one might expect a scaling law of the corresponding structure functions $S_p^L(l) = \langle (\delta_\tau v_i)^p \rangle \sim \tau^{\zeta_p^L}$ within the temporal inertial range of scales it has not yet been clearly observed^{14,15}. The origin of the strong measured intermittency, the very existence of an inertial range of scales, the corresponding scaling exponents, and their relation to Eulerian intermittency are still open issues^{16–18}.

In this paper we measure conditional velocity statistics both in the Eulerian as well as in the Lagrangian frame of reference by means of high-Reynolds number DNS. We approve the experimental results obtained by Gagne et al.¹⁰ and Naert et al.¹⁹ and complement their findings by a detailed scale by scale analysis and an investigation of the statistics of conditioned transverse velocity increments. Furthermore we analyze conditioned Lagrangian increment statistics.

In the next section we briefly present the numerical method. Section III presents the results in the Eulerian frame and section IV those in the Lagrangian frame of reference. Conclusion are summarized in section V.

II. NUMERICS

The numerical simulations were performed by solving the incompressible Navier-Stokes equations

$$\partial_t \mathbf{u} + (\mathbf{u} \cdot \nabla) \mathbf{u} = \mathbf{f} - \nabla p + \nu \Delta \mathbf{u} \quad (6)$$

$$\nabla \cdot \mathbf{u} = 0, \quad (7)$$

in a periodic cube with a pseudo-spectral method using a high-order exponential cut-off^{20,21}.

We parallelize the computations via a pencil geometry by means of the San Diego P3D-FFT²² and explore the BlueGene/P-architecture (the 2048³ simulation was performed on 32k processors). The time integration of the velocity field is done by means of a strongly stable Runge-Kutta third order scheme²³. In order to maintain a statistically stationary flow a forcing \mathbf{f} is applied which keeps constant the modes of the two lowest Fourier-shells. Averages are taken over several statistically independent realizations of the velocity field.

Once a stationary state has been reached 10 Million tracers are seeded into the flow and integrated according to

$$\dot{\mathbf{X}}(\mathbf{x}_o, t) = \mathbf{u}(\mathbf{X}(\mathbf{x}_o, t), t), \quad (8)$$

where $\mathbf{u}(\mathbf{X}, t)$ is the velocity obtained from (6).

In order to obtain the velocity at the particle position from the grid values we use a tri-cubic interpolation²⁴. All relevant quantities such as the gradient of velocity are stored in intervals of 1/7th of the dissipation timescale. The main parameters of all simulations are given in Table I.

III. EULERIAN CONDITIONAL STATISTICS

In this section we present the result on conditioned Eulerian increments statistics. We are going to start with longitudinal increments, followed by transverse increments in the subsequent section.

A. Longitudinal increments

Following the experimental results obtained by Gagne et al.¹⁰ as well as Naert et al.¹⁹, we split our simulation domain in subsets Ω_{ϵ_l} of fixed rate of energy dissipation ϵ_l on a line l defined by (4). On these subsets we consider longitudinal velocity increments $\delta_l^{\parallel} u$ in order to obtain conditional PDFs $P(\delta_l^{\parallel} u | \epsilon_l)$. The standard (unconditioned) PDFs can be recovered by integrating this PDF over all ϵ_l . In agreement with the experimental results we find for a separation l within the inertial range of scales nearly Gaussian statistics for different dissipation rates (see Fig. 1). Also for different scales l we recover

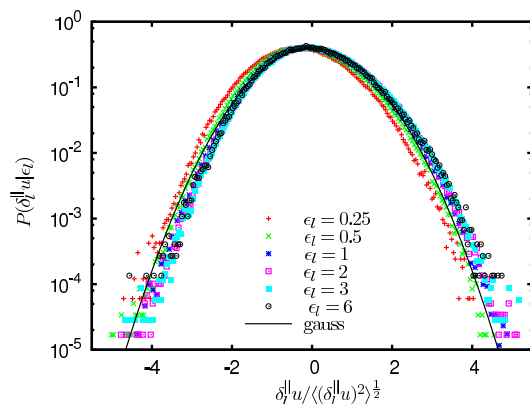


FIG. 1. Conditioned PDFs $P(\delta_l^{\parallel} u | \epsilon_l)$ for different space-averaged dissipation rates ϵ_l for $l = 93\eta$ in comparison to a Gaussian distribution, $\epsilon_l = 1$ corresponds to the most probable energy dissipation rate, the others of multiples of this rate. All PDFs are normalized to unit variance.

Gaussianity (see Fig. 2). The unconditioned PDFs have clearly flatter tails.

As a measure of the deviation from Gaussianity we present in Fig. 3 the flatness $\langle (\delta_l^{\parallel} u)^4 \rangle / \langle (\delta_l^{\parallel} u)^2 \rangle^2$. The figure includes the logarithmic derivative of the third-order structure function $S_3^{\parallel}(l)$ in order to illustrate the inertial

\Re_λ	u_{rms}	ϵ_k	ν	dx	η	τ_η	L	T_L	N^3	N_p
460	0.189	$3.6 \cdot 10^{-3}$	$2.5 \cdot 10^{-5}$	$3.07 \cdot 10^{-3}$	$1.45 \cdot 10^{-3}$	0.083	1.85	9.9	2048^3	10^7

TABLE I. Parameters of the numerical simulations. $\Re_\lambda = \sqrt{15VL/\nu}$: Taylor-Reynolds number, u_{rms} : root-mean-square velocity, ϵ_k : mean kinetic energy dissipation rate, ν : kinematic viscosity, dx : grid-spacing, $\eta = (\nu^3/\epsilon_k)^{1/4}$: Kolmogorov dissipation length scale, $\tau_\eta = (\nu/\epsilon_k)^{1/2}$: Kolmogorov time scale, $L = (2/3E)^{3/2}/\epsilon_k$: integral scale, $T_L = L/u_{\text{rms}}$: large-eddy turnover time, N^3 : number of collocation points, N_p : number of tracer particles.

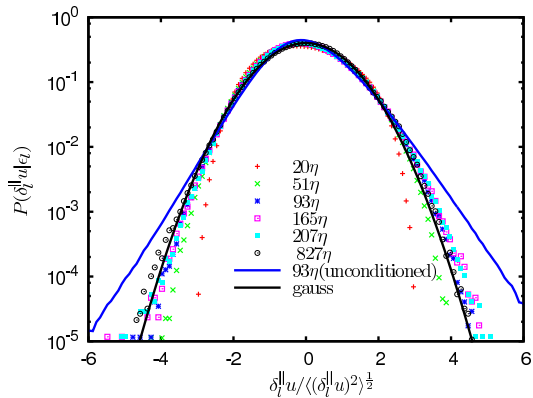


FIG. 2. Conditioned PDFs $P(\delta_l^{\parallel} u | \epsilon_l)$ for different separations l and the most probable value of ϵ , normalized to unit variance

range via its plateau. The PDFs of the conditioned increments (Fig. 2) reach a flatness of approximately three throughout the inertial range of scales.

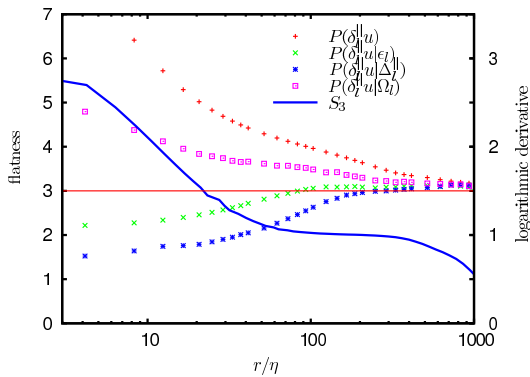


FIG. 3. Flatness factors for conditioned velocity increment PDFs $P(\delta_l^{\parallel} u | \epsilon_l)$, $P(\delta_l^{\parallel} u | \Omega_l)$, $P(\delta_l^{\parallel} u | \Delta_l)$ and the unconditioned PDF $P(\delta_l^{\parallel} u)$, including the logarithmic derivative of the third order structure function S_3^{\parallel} . The horizontal line indicates the flatness of a Gaussian distribution.

For comparison we conditioned the velocity increments on other quantities composed of velocity-gradient tensor elements, namely the vorticity $\boldsymbol{\omega} = \nabla \times \mathbf{u}$ and the longitudinal gradient $\hat{\mathbf{l}} \cdot \nabla \mathbf{u}$. As for the energy dissipation rate

we consider spatial averages of the square of vorticity

$$\Omega_l = \frac{1}{l} \int_0^l ds \nu |\boldsymbol{\omega}(\mathbf{x} + s \hat{\mathbf{l}})|^2. \quad (9)$$

and the square of the longitudinal gradient

$$\Delta_l^{\parallel} = \frac{1}{l} \int_0^l ds \nu |\hat{\mathbf{l}} \cdot \nabla \mathbf{u}(\mathbf{x} + s \hat{\mathbf{l}})|^2. \quad (10)$$

From Fig. 3 one recognizes that the flatness of $P(\delta_l^{\parallel} u | \epsilon_l)$ is closer to a Gaussian distribution over all scales than $P(\delta_l^{\parallel} u | \Omega_l)$ or $P(\delta_l^{\parallel} u | \Delta_l)$. It is interesting to remark that the integral of the longitudinal gradient over l is the longitudinal increment. That the energy dissipation rate ϵ_l nevertheless works better than this longitudinal gradient implies that correlations of the form $\partial_j u_i \partial_i u_j$ with $i \neq j$ are essential in the condition (3) and in the RSH (2).

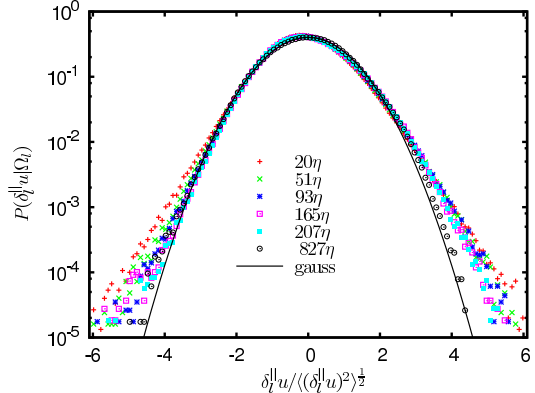


FIG. 4. Conditioned PDFs $P(\delta_l^{\parallel} u | \Omega_l)$ for different separations l in comparison to a Gaussian distribution, normalized to unit variance

The flatness of the PDFs conditioned to the scale-averaged energy dissipation rate come closest to the Gaussian value. However, from Fig. 4 one observes that the PDFs conditioned on Ω_l are also nearly scale-invariant but not exactly Gaussian.

Whether longitudinal increments are conditioned on the energy-dissipation or vorticity yields quasi-identical results. With respect to the slightly smaller flatness of the former one can conclude that longitudinal increment statistics is coupled more closely to the scale averaged

energy dissipation rate than to the vorticity. This is important for diverse models such as the She-Lévêque model²⁵, where physical reasoning is based on the one hand on the energy dissipation rate and the RSH and on the other hand on the dimensionality of the coherent structures of vorticity. This question is also closely related to the issue of different scaling laws for longitudinal and transverse structure functions as we will explain in the next section.

We conclude this section on longitudinal increments by an examination of the corresponding conditioned structure functions S_{p,ϵ_l} . From the scale-invariant PDFs in Fig. 3 we expect them to follow the linear K41-scaling law $p/3$ within the inertial range. Indeed, as shown in Fig. 5, the conditioned structure functions follow Kolmogorov's prediction while the unconditioned higher-order functions exhibit lower plateaus expressed by a non-zero μ_p in (1).

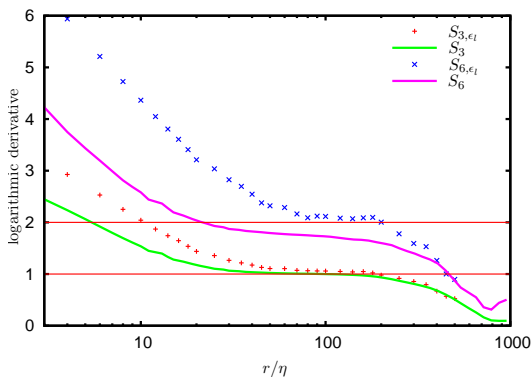


FIG. 5. Logarithmic derivative of the conditioned and unconditioned longitudinal velocity structure function of order $p = 3$ and $p = 6$, lines indicate the K41-prediction

B. Transverse increments

In analogy to the RSH for the longitudinal velocity increments Chen et al.²⁶ proposed a refined self-similarity hypothesis for the transverse velocity increments (RSHT). This relation of the scale-averaged square of vorticity and the transverse velocity increments reads

$$\delta_l^\perp u = \beta_2 (\Omega_l l)^{\frac{1}{3}}, \quad (11)$$

where β_2 is a statistical variable independent of l and Ω_l , given by (9).

Following Chen et al. it is reasonable to look in the transverse case at the statistics of velocity increments conditioned to Ω_l , namely the PDFs $P(\delta_l^\perp u | \Omega_l)$. They are scale-invariant and only slightly flatter than Gaussian PDFs (see Fig. 6). As in the case of longitudinal increments one can ask how other conditions such as the energy dissipation rate perform compared to ϵ_l . The PDFs conditioned on ϵ_l shown in Fig. 7 are indistinguishable

from the PDFs conditioned on the vorticity Ω_l . From this point of view it is impossible to conclude whether ϵ_l or Ω_l is the better condition for the transverse fluctuations. In order to make a more precise statement on the

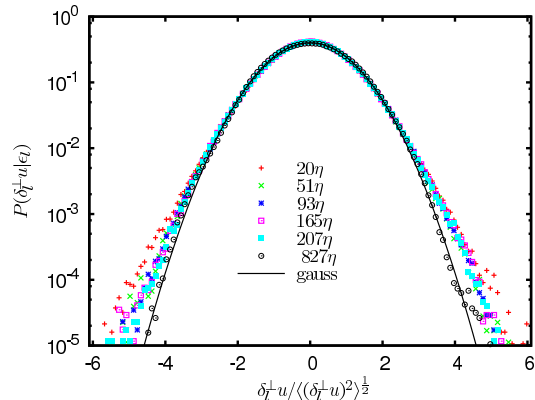


FIG. 6. Conditioned PDFs $P(\delta_l^\perp u | \epsilon_l)$ for different separations l in comparison to a Gaussian distribution, normalized to unit variance

difference between these two conditions it is helpful to look at the flatness in Fig. 8. From this we conclude that

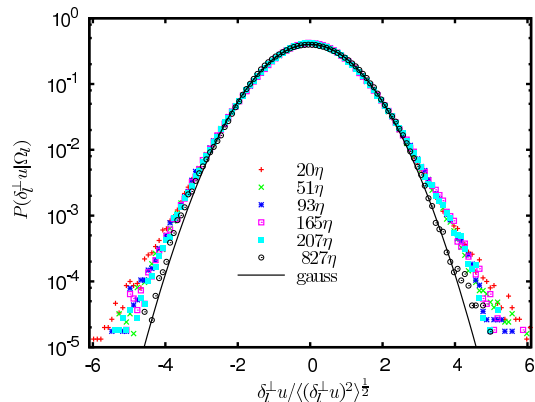


FIG. 7. Conditioned PDFs $P(\delta_l^\perp u | \Omega_l)$ for different separations l in comparison to a Gaussian distribution, normalized to unit variance

conditioning to ϵ_l or Ω_l yields quasi-identical results and surprisingly $P(\delta_l^\perp u | \epsilon_l)$ are even slightly more Gaussian than $P(\delta_l^\perp u | \Omega_l)$. The averaged transverse gradient

$$\Delta_l^\perp = \frac{1}{l} \int_0^l ds \nu |\hat{l} \times \nabla \mathbf{u}(\mathbf{x} + s \hat{l})|^2. \quad (12)$$

reduces the flatness less than the two other conditions. The transverse structure functions are shown in Fig. 9. As expected, we find that the conditioned ones follow the K41 prediction with the inertial range of scale while the high-order unconditioned functions have significantly lower plateaus.

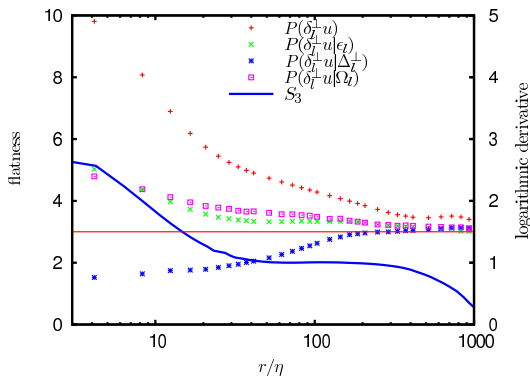


FIG. 8. Flatness factors of the conditioned PDFs $P(\delta_l^\perp u|\Omega_l)$, $P(\delta_l^\perp u|\epsilon_l)$, $P(\delta_l^\perp u|\Delta_l^\perp)$ and unconditioned $P(\delta_l^\perp u)$, including the third order transverse structure function S_3^\perp

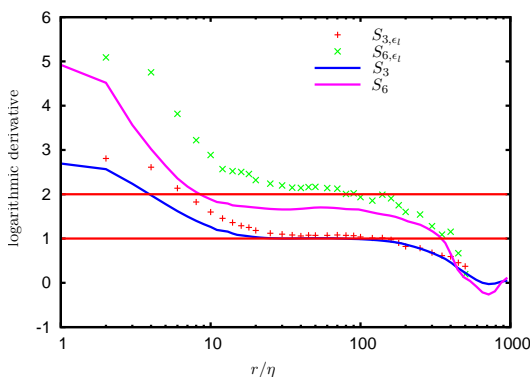


FIG. 9. Logarithmic derivative of the conditioned and unconditioned transverse velocity structure function of order $p = 3$ and $p = 6$, lines indicate the Kolmogorov prediction

IV. LAGRANGIAN CONDITIONAL STATISTICS

After having computed statistics in the Eulerian framework we now consider velocity increments (5) in the Lagrangian frame of reference. The Lagrangian analog to the RSH might be labeled the Lagrangian refined self-similarity hypothesis (LRSH) and reads

$$\delta_\tau v_i = \beta_L (\tau \epsilon_\tau)^{1/2}, \quad (13)$$

where the local energy dissipation rate (3) is averaged along a particle trajectory according to

$$\epsilon_\tau = \frac{1}{\tau} \int_0^\tau \epsilon(\mathbf{X}(\mathbf{x}_0, t)) dt. \quad (14)$$

However, one can question whether ϵ_τ is the correct quantity appearing in (13). Benzi et al.²⁷ examined this relation by means of the assumption of extended self-similarity and found that ϵ_τ rather than the averaged square of vorticity

$$\Omega_\tau = \frac{1}{\tau} \int_0^\tau |\boldsymbol{\omega}(\mathbf{X}(\mathbf{x}_0, t))| dt.$$

is the correct quantity in (13). Yu et al.²⁸ conditioned the velocity increments on a spatially averaged energy dissipation rate at one foot-point of the increments.

In this work we stick to trajectory-averaged conditions and propose yet another one for Lagrangian increment statistics. In order to motivate this on dimensional grounds we recall that Eulerian increments $(u_i(l \mathbf{e}_j) - u_i(0))/l$ tend to spatial derivatives $\partial_j u_i$ of the velocity field in the limit $l \rightarrow 0$. Those derivatives appear in the local energy dissipation rate (3). Instead, Lagrangian increments $(u_i(\tau) - u_i(0))/\tau$ tend to the fluid-particle acceleration in the limit $\tau \rightarrow 0$ which involve a term $u_j \partial_j u_i$. We therefore propose to replace (14) by

$$\epsilon_\tau^L = \frac{1}{2} \int dt \sum_{i,j} [u_j \partial_j u_i + u_i \partial_i u_j]^2 \quad (15)$$

in the LRSH (13).

The calculation of ϵ_τ , Ω_τ , and ϵ_τ^L for a given time lag τ is done by averaging the local quantities over all stored points along the particle trajectory. We achieved converged statistics by taking the average over 10 Million particles and several large-eddy turn-over times.

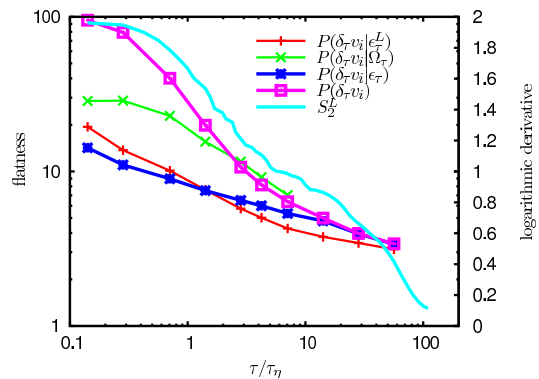


FIG. 10. Flatness factors of the conditioned velocity increment PDFs $P(\delta_\tau v_i|\epsilon_\tau)$, $P(\delta_\tau v_i|\Omega_\tau)$ and $P(\delta_\tau v_i|\epsilon_\tau^L)$ as well as of the unconditioned PDF $P(\delta_\tau v_i)$ together with the logarithmic derivative of S_2^L

In Fig. 10 we compare the flatness of velocity increment PDFs conditioned on ϵ_τ , Ω_τ , and ϵ_τ^L . We added the logarithmic derivative of the second order Lagrangian structure function $S_2^L(l) = \langle (\delta_\tau v_i)^2 \rangle$ in order to clarify three different ranges of scales: The dissipative scales up to $\tau \approx 1$, the inertial ones $1 < \tau < 60$, followed by the large scales. If we restrict our attention to the inertial range we observe that the flatness is most efficiently reduced by ϵ_τ^L . Also the trajectory integrated energy dissipation rate ϵ_τ diminishes significantly the flatness while the integrated vorticity Ω_τ has a negligible effect. This indicates that ϵ_τ^L might be a more appropriate condition than ϵ_τ .

The corresponding conditioned increment PDFs are labeled $P(\delta_\tau v_i|\epsilon_\tau)$ and show in Fig. 11. The PDF corresponding to the shortest time-lag considered is reason-

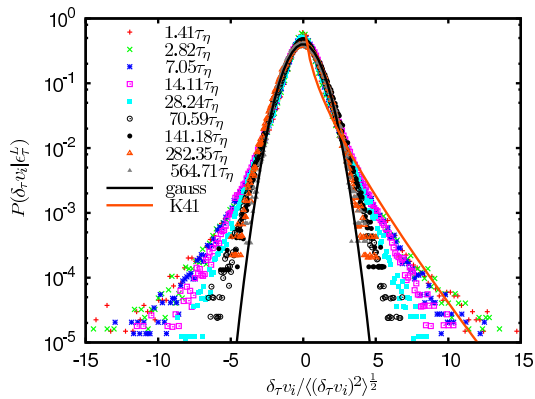


FIG. 11. Conditioned PDFs $P(\delta_\tau v_i | \epsilon_\tau^L)$ for different time lags τ in comparison to a Gaussian distribution and to the K41-prediction for the PDF of acceleration, normalized to unit variance

ably well described by the K41-acceleration PDF¹⁶

$$P(a) = (a/b)^{-5/9} \exp[-0.5(a/b)^{8/9}]/c \quad (16)$$

normalized to unit-variance with $a = 0.48$ and $b = 2.72$. This PDF is the Lagrangian analogon to a Gaussian distribution for Eulerian velocity gradients.

It is important to note that contrarily to the results in Eulerian setup the conditioned Lagrangian PDFs $P(\delta_\tau v_i | \epsilon_\tau^L)$ (see Fig. 11) are still scale-dependent. One notes a transition from stretched tails (K41-prediction) for short time-lags to Gaussian PDFs (uncorrelated statistics) for time lags of the order of the integral time scale. This implies that Lagrangian increment statistics is 'naturally' scale dependent.

As can be seen from the unconditioned structure function in Fig. 10, Lagrangian structure functions do not show a clear scaling law at today accessible Reynolds numbers. We therefore refer to relative structure functions $S_p(S_2)$. In the computation of the conditioned structure functions we fixed one ϵ_τ^L for all increments τ . In Fig. 12 their logarithmic derivatives are shown which clearly change under the condition ϵ_τ^L . There are two major differences between the conditioned and unconditioned functions. The first concerns intermittency: The conditioned functions have larger values than the unconditioned ones. We observe a value of approximately 1.43 which is close to the K41 prediction of 1.5. This implies that intermittency is significantly reduced on subsets $\Omega_{\epsilon_\tau^L}$. A second feature of Lagrangian increment statistics is the so called bottleneck around a few τ_η . It has been attributed to the characteristic trajectories (spirals) of tracers in the vicinity of coherent vortex filaments. This bottleneck in the local slope is absent once velocity increments are conditioned (see again Fig. 12), which means that their scaling range is enlarged. Its origin is supposed to be in the coexistence of two different power-laws. The first related to dissipative effects and the second to inertial range physics²⁹. An insufficient

separation of dissipative and inertial scales might lead to the observed dip in the local slope of structure functions. Interestingly, this bottleneck is negligible in the case of conditioned structure functions. This implies that it is due to a mixture of statistics from different subset $\Omega_{\epsilon_\tau^L}$.

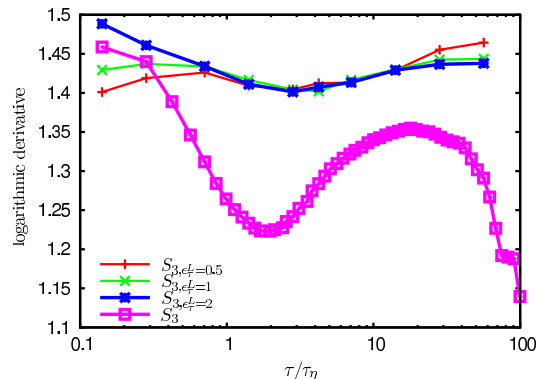


FIG. 12. Logarithmic derivatives of relative Lagrangian velocity structure function. $\epsilon_\tau^L = 1$ corresponds to the one with the most statistics

V. CONCLUSION

This work investigates the statistics of Eulerian and Lagrangian velocity increments when conditioned to different scale-averaged quantities such as the energy dissipation rate, the square of vorticity or the velocity gradient. In the case of Lagrangian increments we propose a novel condition dimensionally related to the acceleration of fluid elements.

Considering Eulerian statistics we find that longitudinal as well as transverse increment PDFs are Gaussian shaped with flatness factors close to three when conditioned to the scale-averaged energy dissipation rate. The averaged vorticity produces slightly flatter tails while the longitudinal and transverse velocity gradient perform significantly worse. Therefore, there is no preferential link of transverse increments and vorticity as of longitudinal increments and energy dissipation rate which is important for models of intermittency. Conditional structure functions show clear K41-scaling within the inertial range of scales.

Considering Lagrangian statistics we investigated velocity increments conditioned to trajectory-averaged quantities such as the energy dissipation rate, the vorticity and a novel condition. The latter is motivated by dimensional arguments. Conditioning to the dissipation rate and to the novel condition yields flatnesses of the increment PDFs much smaller than without conditioning. More precisely, the conditioned PDF of the shortest increment considered agrees reasonably well with the K41-prediction for the PDF of acceleration. Within the inertial range of scales the flatnesses of PDFs under the novel

condition are even smaller than the flatness of PDFs conditioned on the averaged energy dissipation.

Conditioned and unconditioned Lagrangian structure functions differ significantly. First, conditioning yields quasi-K41 scaling exponents. Secondly, the characteristics bottleneck of the unconditioned functions at the onset of the inertial range disappears once conditioned.

ACKNOWLEDGMENTS. This study benefited from fruitful discussions with A. Naert and J. Bec. Access to the IBM BlueGene/P computer JUGENE at the FZ Jülich was made available through the 'XXL-project' of HBO28 and partly through project HBO36. This work benefited from support through DFG-FOR1048

- ¹U. Frisch, *Turbulence* (Cambridge, Cambridge University Press, 1995).
- ²A. Tsinober, *An Informal Conceptual Introduction to Turbulence: Second Edition of An Informal Introduction to Turbulence* (Springer, Netherlands, 2009).
- ³A. N. Kolmogorov *C. R. Acad. Sci. URSS*, **32**, 19 (1941).
- ⁴B. Dhruva, Y. Tsuji, and K. Sreenivasan, "Transverse structure functions in high-Reynolds-number turbulence," *Physical Review E*, **56**, 4928–4930 (2000).
- ⁵T. Zhou, Z. Hao, L. P. Chua, and S. C. M. Yu, "Scaling of longitudinal and transverse velocity increments in a cylinder wake," *Physical Review E*, **71**, 066307 (2005).
- ⁶S. Grossmann, L. Detlef, and A. Reeh, "Different intermittency for longitudinal and transversal turbulent fluctuations," *Physics of Fluids*, **9**, 3817 (1997).
- ⁷K. Gernaschewski and R. Grauer, "Longitudinal and transversal structure functions in two-dimensional electron magnetohydrodynamic flows," *Physics of Plasmas*, **6**, 3788 (1999).
- ⁸R. Grauer, H. Homann, and J.-F. Pinton, "On longitudinal and transverse structure functions in high reynolds-number turbulence," *in preparation*.
- ⁹A. N. Kolmogorov *J. Fluid Mech.*, **13**, 82 (1962).
- ¹⁰Y. Gagne, M. Marchand, and B. Castaing, "Conditional velocity pdf in 3-d turbulence," *J. Phys. II France*, **4**, 1–8 (1994).
- ¹¹S. Ott and J. Mann, "An experimental investigation of the relative diffusion of particle pairs in three-dimensional turbulent flow," *Journal of Fluid Mechanics*, **422**, 207–223 (2000).
- ¹²A. L. Porta, G. A. Voth, A. M. Crawford, J. Alexander, and E. Bodenschatz, "Fluid particle accelerations in fully developed turbulence," *Nature*, **409**, 1017–1019 (2001).
- ¹³N. Mordant, P. Metz, O. Michel, and J. F. Pinton, "Measurement of lagrangian velocity in fully developed turbulence," *Phys. Rev. Lett.*, **87**, 214501 (2001).
- ¹⁴P. K. Yeung and M. S. Sawford, "Reynolds number dependence of lagrangian statistics in large numerical simulations of isotropic turbulence," *J. of Turbulence*, **7**, 1–12 (2006).
- ¹⁵L. Biferale, E. Bodenschatz, M. Cencini, A. Lanotte, N. T. Ouellette, F. Toschi, and H. Xu, "Lagrangian structure functions in turbulence: A quantitative comparison between experiment and direct numerical simulation," *Phys. Fluids*, **20**, 065103 (2008).
- ¹⁶L. Biferale, G. Boffetta, A. Celani, B. J. Devenish, A. Lanotte, and F. Toschi, "Multifractal statistics of lagrangian velocity and acceleration in turbulence," *Phys. Rev. Lett.*, **93**, 4502 (2004).
- ¹⁷O. Kamps, R. Friedrich, and R. Grauer, "An exact relation between eulerian and lagrangian velocity increment statistics," *Phys. Rev. E*, **79**, 066301 (2009).
- ¹⁸H. Homann, O.Kamps, R. Friedrich, and R. Grauer, "Bridging from eulerian to lagrangian statistics in 3d hydro- and magnetohydrodynamic turbulent flows," *New J. Phys.*, **11**, 073020 (2009).
- ¹⁹A. Naert, B. Castaing, B. Hbral, and J. Peinke, "Conditional statistics of velocity fluctuations in turbulence," *Physica D*, **113**, 73–78 (1998).
- ²⁰T. Y. Hou and R. Li, "Computing nearly singular solutions using pseudo-spectral methods," *J. Comp. Phys.*, **226**, 379–397 (2007).
- ²¹T. Grafke, H. Homann, J. Dreher, and R. Grauer, "Numerical simulations of possible finite time singularities in the incompressible euler equations: comparison of numerical methods," *Physica D*, **237**, 1932–1936 (2008).
- ²²"Parallel 3d fast fourier transforms (p3dffft)." <http://www.sdsc.edu/us/resources/p3dffft>.
- ²³C. Shu and S. Osher, "Efficient implementation of essentially non-oscillatory shock-capturing schemes," *J. Comput. Phys.*, **77**, 439–471 (1988).
- ²⁴H. Homann, J. Dreher, and R. Grauer, "Impact of the floating-point precision and interpolation scheme on the results of dns of turbulence by pseudo-spectral codes," *Comput. Phys. Comm.*, **177**, 560–565 (2007).
- ²⁵Z.-S. She and E. Lévéque, "Universal scaling laws in fully developed turbulence," *Phys. Rev. Lett.*, **72**, 336–339 (1994).
- ²⁶S. Chen, K. Sreenivasan, M. Nelkin, and N. Cao, "Refined similarity hypothesis for transverse structure functions in fluid turbulence," *Phys. Rev. Lett.*, **79**, 2253 (1997).
- ²⁷R. Benzi, L. Biferale, E. Calzavarini, D. Lohse, and F. Toschi, "Velocity-gradient statistics along particle trajectories in turbulent flows: The refined similarity hypothesis in the Lagrangian frame," *Physical Review E*, **80**, 066318 (2009).
- ²⁸H. Yu and C. Meneveau, "Lagrangian Refined Kolmogorov Similarity Hypothesis for Gradient Time Evolution and Correlation in Turbulent Flows," *Physical Review Letters*, **104**, 084502 (2010).
- ²⁹ICTR, A. Arneodo, R. Benzi, J. Berg, L. Biferale, E. Bodenschatz, A. Busse, E. Calzavarini, B. Castaing, M. Cencini, L. Chevillard, R. Fisher, R. Grauer, H. Homann, D. Lamb, A. Lanotte, E. Leveque, B. Luethi, J. Mann, N. Mordant, W. Mueller, S. Ott, N. Ouellette, J. Pinton, S. Pope, S. Roux, F. Toschi, H. Xu, and P. Young, "Universal intermittent properties of particle trajectories in highly turbulent flows," *Phys. Rev. Lett.*, **100**, 254504 (2008).